La mer 34: 183–191, 1996
Société franco-japonaise d'océanographie, Tokyo

The stratification variations during spring and neap tidal periods in Deukryang Bay, Korea

Byung-Gul LEE*, Tetsuo YANAGI**, Hidetaka TAKEOKA**
and Kyu-Dae CHO***

Abstract: The stratification-destratification (SD) phenomenon in Deukryang Bay, Korea was studied based on the data of wind speed, heat flux through the sea surface and tidal current amplitude. To find out the main factors causing SD, we introduce the rate of energy balance of the surface heat flux, tidal and wind stirring proposed by SIMPSON and HUNTER (1974). The calculated energy of three terms are compared, in which energy of wind stirrin effect was one order smaller than that of heat flux and the tidal stirring. Using the results, we implement time integration of the potential energy with the several ε values (tidal mixing efficiency) of 0.010~0.014 at interval 0.001 and with wind speeds of 1.5 and 2.0 times larger than observed values at land. It shows that the variation of SD phenomeenon in the bay mainly depends on tidal stirring and sea surface heating in summer.

1. Introduction

Many oceanographers have studied stratification-destratification (SD) phenomenon during spring-neap tidal cycle (GRIFFIN and LEBLOND, 1990; MACKAY *et al.*, 1990; LARGIER and TALJAARD, 1991) since SIMPSON and HUNTER (1974) proposed the governing equation on the balance between the time rate of change of the potential energy in a unit water columm.

Most of the study area, however, was confined in a coastal zone and estuaries associated with fresh river water discharge or high salinity area. Basically they tried to explain thee temporal variation of a front formed by the horizontal juxtaposition of two distinct water masses and the interaction between the different water masses.

SAMARASINGHE (1989) pointed out temporal changes of salt-wedge movement of the whole domain during spring-neap tidal cycle at the Shark Bay in the Australian Bight, and explained such phenomena based on a density current effect. However, he did not show the critical changes of stratification during spring and neap tidal periods in the day and did not estimate the relationship of other environmental factors.

In Korea, there are so many bays in the southern part of the country and their sizes are mostly less than 1000 km^2, where tidal current is predominant and affects oceanic phenomena in the whole domain of the bays. The Deukryang Bay, one of such bays is a semi-enclosed bay with three open channels. The area is approximately 374.4 km^2 and the average depth 7.5 m (Fig. 1). The eastern part of the bay dips steeply about 30 m while depth decreases slowly on the western part less than 5 m depth.

Tidal elevation ranges in the bay are less than 2 m and the tidal current amplitude from 0.2 m/sec in neap tide to 0.6 m/sec in spring tide in which semi-diurnal components are dominant (LEE, 1992).

The objectives of this paper are firstly to show the drastic changes of SD phenomena during short periods between spring-neap tidal cycle, and second we check the magnitudes and variations of wind speed, sea surface heat flux and tidal current amplitude. Finally, we estimate the budget of potential energy from

* Department of Civil Ocean Engineering, Cheju National University, Cheju 690-756, Korea
** Department of Civil and Ocean Engineering, Ehime University, Bunkyo 3, Matsuyama 790, Japan
*** RCOID, National Fisheries University of Pusan, Pusan 608-737, Korea

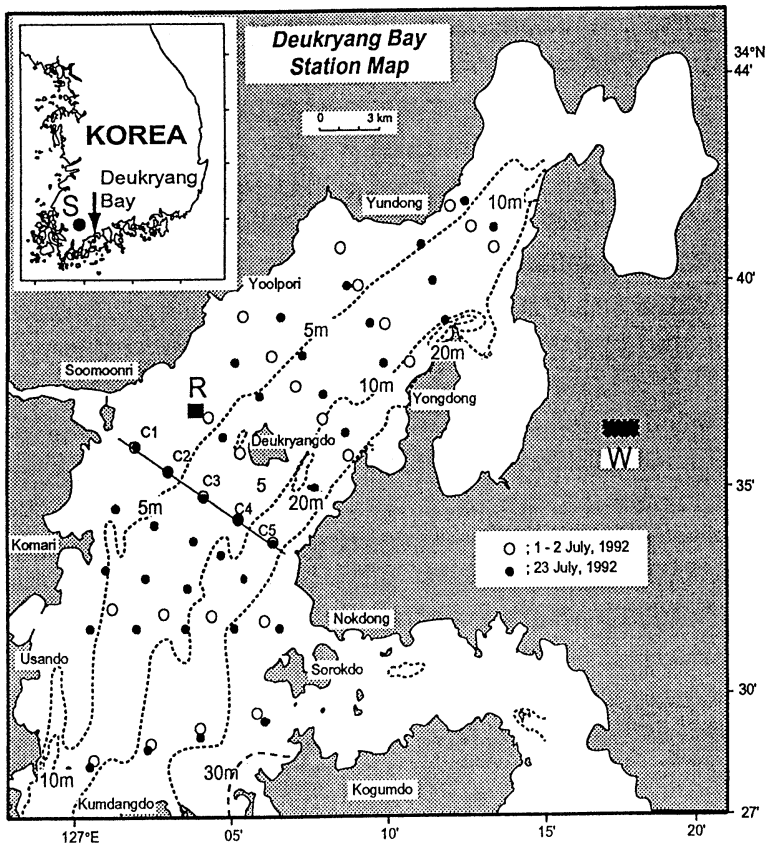

Fig. 1. Location of the Deukryang Bay and obervation points in 1–2 July and 23 July, 1992. S denoted solar radiation station, R and W are current mooring and wind speed stations.

observed data, in addition to prediction the beginning and the ending time of SD phenomenon in summer.

2. Observation results during spring and neap tidal periods

We observed temperature and salinity twice in 1–2 July (spring) and 23 July (neap), 1992, respectively. Three selected stations were shown in Fig. 1 in which the first observation points were 27 and the second were extended to 37 for more detail observation so that the station positions between the first and the second were different except transect C. The mooring station of current meter was R and the wind speed was W, and the solar radiation S was observed at Kwangju City located for from the study area about 100 km since there is no meteorological observation center including the solar radiation data near the study area.

Figure 2 presents T-S diagrams for the observation data at all stations of surface and bottom during the spring and the neap tidal periods. In the figure, the salinity variations were less than 1 PSU at twice observations and appeared to be insignificant compared to the temperature ones. The temperature in spring tide, ranged from 19 to 25℃ and the character of water mass in bottom and surface layers is almost the same while in neap tide the temperature from 20 to 27℃, water masses are separated into two parts. The intensities of the surface and bottom temperature gradients were so much different between neap and spring tidal periods.

Figure 3 was constructed to present vertical temperature, salinity and density distributions, along section C. The data indicated the drastic changes of vertical structures between two observation periods. From the figure, the vertical

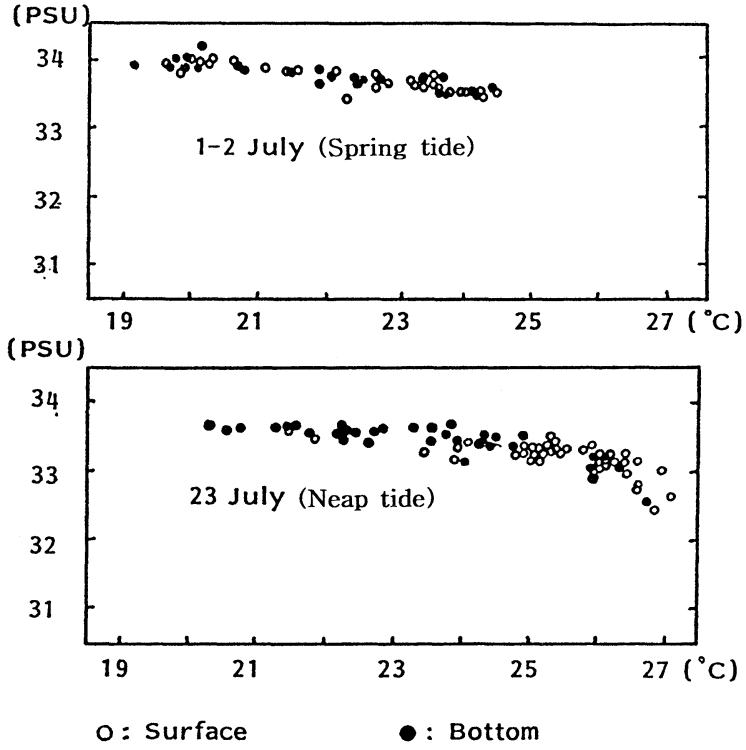

Fig. 2. The variations of temperature and salinity from bottom to surface (T-S diagram) during spring and neap tidal cycle.

temperature and density gradients in neap tide showed strong stratification while in spring tide vertically well mixed. The temperature variations at spring and neap tides are larger than the salinity ones so that the temperature is more effective to form vertical stratification in the periods. Although the partially mixed form at C1, C2, and C3 appeared during neap tide, it looks like local phenomenon since it occurred only in shallow region limited less than 5 m depth. Regarding this, SD characteristics in the bay can be mainly controlled by the the heat flux through the sea surface, tidal and wind stirring effects.

3. Heat Flux, Wind and Current Variations during Spring and Neap Tidal Periods

Oceanographical and meteorological data were compared for estimating the variability of SD phenomenon during spring-neap tidal cycle. Wind speed, surface heat flux, and tidal current variations are shown in Fig. 4.

The heat flux was calculated based on the method of YANAGI (1982) and GILL (1984), and daily mean variation of sea surface water temperature was calculated from linear interpolation and extrapolation methods using two times observation on 1–2 July and 23 July. In Fig. 4, the wind speed ranges approximately from 1 to 2 m/sec, the heat flux from 0 to 200 Watt/m^2, the tidal current amplitude from 0.1 to 0.6 m/sec. Wind speed from 21 June to 23 July are not strong and not changed comparing to other factors. Moreover, the wind in the period of strong stratification was stronger than that of vertically well mixed condition. It gives an account of that the wind stirring effect for the stratification may be not the main factor in the bay.

The fluctuation of the heat flux was very large in spite of monthly average of 124 Watt /m^2, sometimes zero values happened because of a lot of cloud that prohibits the solar heating through the sea surface.

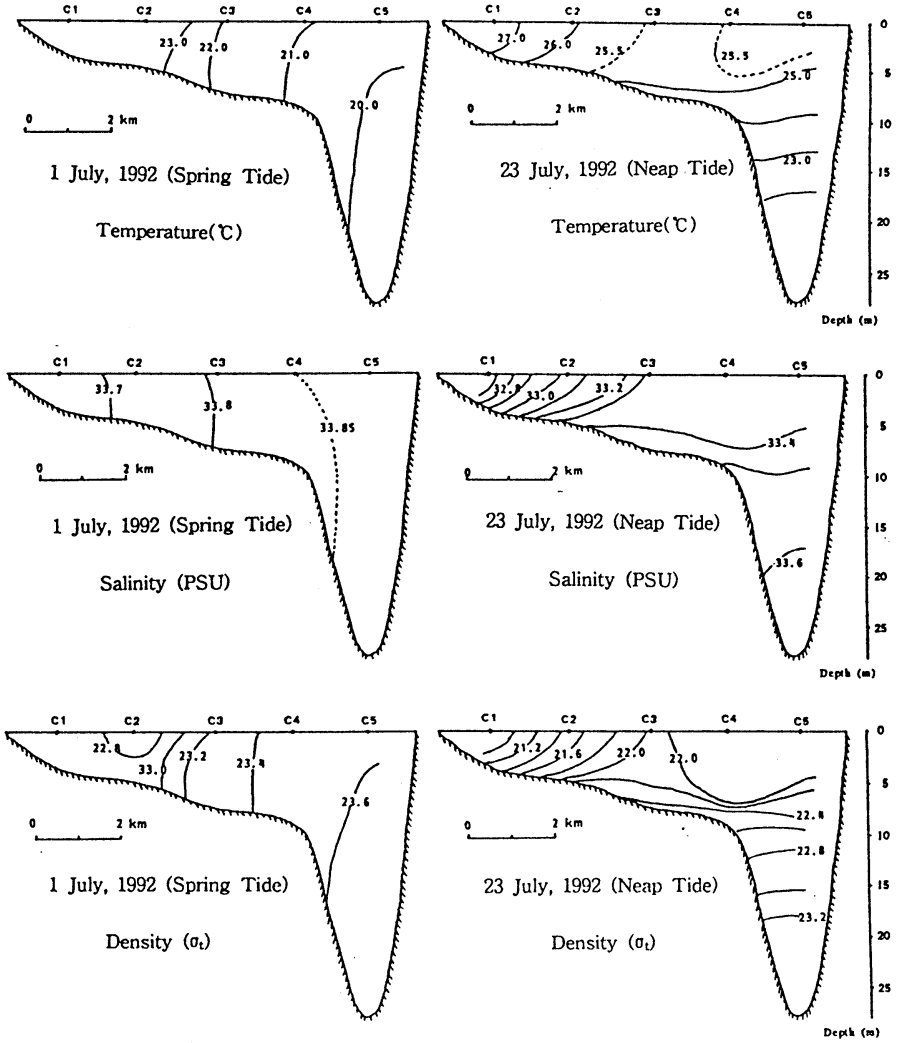

Fig. 3. hydrographic profile during spring and neap tidal cycle at typical central part of the Deukryang Bay along Section-C.

The stick current velocity diagram in the figure shows the manifest fluctuations of tidal current amplitude, particularly M_2 tidal current was dominated. The current amplitude was the largest in the first observation time while in the second the velocity was the lowest. From 13 to 20 July, the current was relatively weaker than that during the former spring period so that presumably comparatively low tidal mixing occurred at this period.

4. The budget of potential energy during spring and neap tidal periods

It was clear that the SD phenomenon during spring-neap tidal cycle existed in Deukryang Bay from previous results. We showed that is phenomenon as related to mostly the heat flux and the tidal current amplitude from data analysis.

To estimate the variation of stratification due to three factors, we used basically the simple potential energy arguments given by Simpson and HUNTER (1974), ELLIOTT (1991), and TAKEOKA *et al.* (1993) who studied at

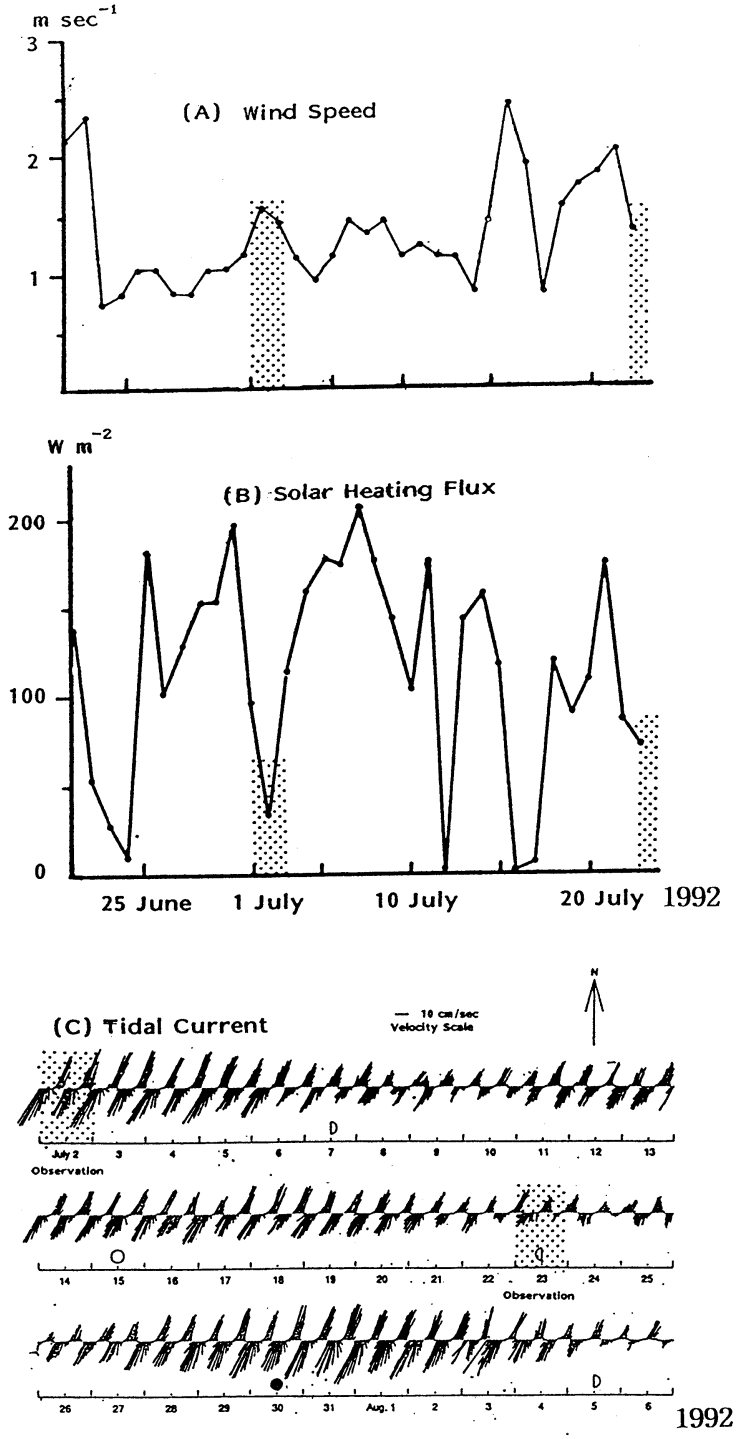

Fig. 4. The time variations of the wind speed, the heat flux and tidal current amplitute. ⁘ : Observation periods of hydrographic data.

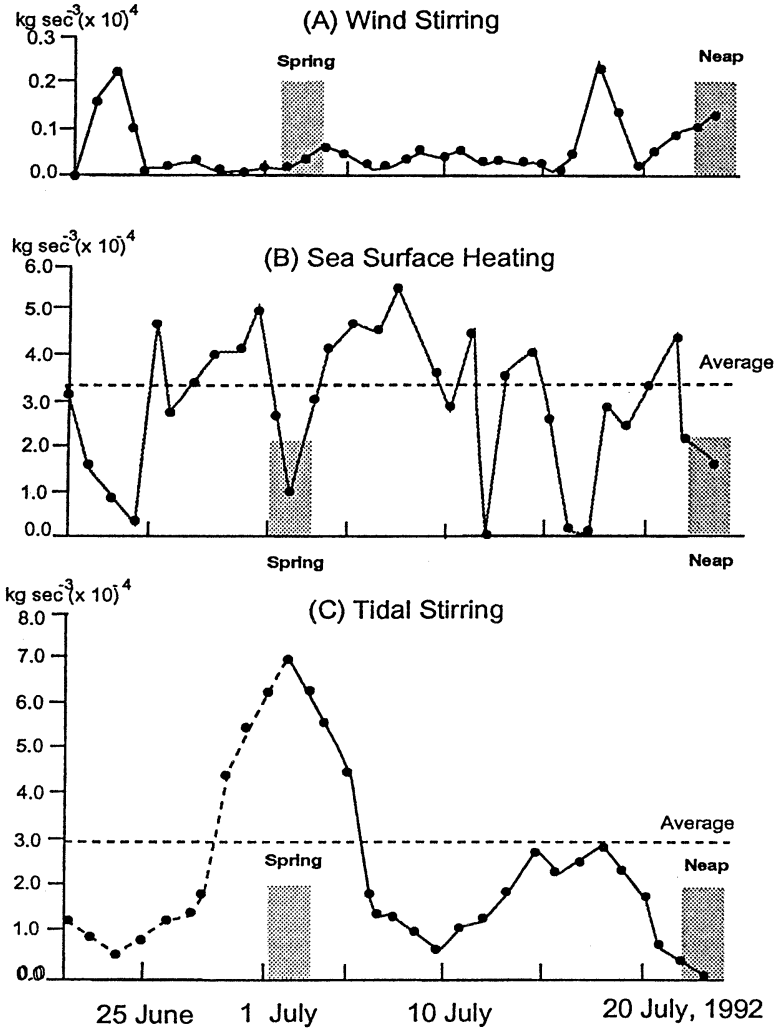

Fig. 5. The time variations of the rate of potential energy anomaly of a water column based on Fig. 4. ⁘ : Observation periods of hydrographic data.

European Shelf and at Bungo Channel in Japan.

If we assume that the total rate of change in potential energy of a water column is only influenced by the wind and the tidal stirring and the sea surface heating, the daily mean rate of change in the energy will be given by (ELLIOTT, 1991)

$$\frac{dE}{dt} = \frac{g\alpha}{2C_\rho} Q_T H - eC_A \rho_a W^3 - \varepsilon C_D \rho_W U^3 \cdots\cdots (1)$$

Here, E is the potential energy of a water column. The first term in the right hand of equation (1) is the loss of potential energy by the surface heating, the second and the third are the gain of potential energy by the wind and tidal current, where g is gravitational acceleration, α is thermal expansion coefficient, ρ_a and ρ_w are air and water density, e and ε are efficiencies of surface and bottom mixing process, C_A and C_D represent the surface and bottom drag coefficients. W is wind speed, U is the absolute tidal current speed. H is water depth (10 m). If the right side of equation (1) is positive, stratification is intensified, and if it is negative, the stratification is weakened.

In calculation procedure of above equation, we used tentatively 0.015 ε value proposed by YANAGI and TAMARU (1990) because they successfully applied this value to Bungo Channel, Japan. C_D and C_A are given as 0.0025 and 0.000065 by SIMPSON and BOWERS (1981). The tidal energy values from 20 to 30 June are extrapolated assuming that tidal change pattern from 20 to 30 June is the same as the pattern from 1 to 10 July because of the symmetric characteristics of tidal current amplitude in time.

The calculated results are shown in Fig. 5. As we expected previously, the wind stirring effect is approximately one order of magnitude smaller than the surface heating and the tidal stirring ones. As considering the rate of potential energy derived by wind stress, we argue that the wind effect in summer can be omitted for analyzing SD phenomenon during the observation period. Comparing the energy of the tidal stirring to the surface heating, during the first spring tidal period approximately from 27 June to 5 July, the tidal energy was larger than the heating energy while in the second spring tide of middle of July, the tidal energy was similar to the heating one in which it seems to be impossibel to destroy the stratification already made by sea surface heating. Therefore, the stratification of the first neap tide from 7 to 13 July may also be weaker than that of second neap tide. Possibly, destratification sustained from end of June to early of July, and stratification became to be formed from early July if the surface heating was continually stable.

5. Discussion

Our hydrographic data of Deukryang Bay showed critical changes of vertical structure of temperature, salinity and density between spring and neap tidal periods. As we analyzed meteorological and oceanographical data using three energy equation, it was found that the tidal stirring and the sea surface heating played important roles for the stratifying and mixing processes while wind stirring effect was one order smaller than the previous two factors. However, for more accurate estimates of the effects of sea surface heating and wind and tidal stirring in the bay, we tried to undertake integrate of the rate of potential energy variation between spring-neap tidal cycle, and then estimate the stratification intensity quantitatively.

The integral equation of (1) can be presented as following equation,

$$E_c = \int_{t1}^{t2} [\frac{ga}{2C_D} Q_T H - eC_A \rho_a W^3 - \varepsilon C_D \rho_W U^3] dt \quad \cdots\cdots(2)$$

where tl is ths start time of observation, 1 July, and $t2$ is the end time of observation, 23, July. E_c is the calculated potential energy anomaly. In order to find out an optimal ε values for the Deukryang Bay, equation (2) following several ε values of 0.010~0.014 at 0.001 interval was calculated and its results were compared with the observed value in Table 1.

To compare the calculated result to the observed one, the potential energy anomaly E_0 of observation data was calculated by the following equation (Bowden, 1984) :

$$E_O = \int_{-h}^{O} [\rho - \bar{\rho}] gz \; dz \cdots\cdots(3)$$

where $\bar{\rho} = \frac{1^O}{h_h} \int \rho dz$

ρ is a density at a depth z, $\bar{\rho}$ is averaged density of a total water column. In the calculation, the data of section C located at the nearest stations from the current meter mooring were averaged.

We also showed, in Table 1, the potential energy variations according to the several wind speed conditions, because following YANAGI (1980) and IMANUKI, the wind speed at the sea surface is larger than that at land by about 1.5 or 2 times due to surface roughness differences. In Table 1, W_f is the ratio of an presumed wind velocity at the sea (W_S) and an observed wind velocity at the land (W_M). In the table, the calculated potential energy was very simliar to the observed one in the cases where W_f=1.0 and ε =0.014, W_f=1.5 and ε =0.012, and W_f =2.0 and ε =0.010.

Figure 6 indicates the potential energy variation selected in the case of ε =0.014. The start time tl was 1 July. From the figure, we know that the heating energy was larger than the wind and tidal energy from 5 July. The figure also shows that the stratification gradually

Table 1. The Potential Energy Anomaly Changes for the Coefficients of Tidal Efficiency and Wind Speed (W_M is observation wind at land, Ws is assumed wind at sea) Unit : kg sec^{-2}

	Model						Obser.
ε Value / Wf(=Ws/W_M)	0.010	0.011	0.012	0.013	0.014	0.015	
1.0	262.66	241.84	221.73	201.62	181.51	162.60	194.56
1.5	238.02	217.91	197.80	177.69	157.58	139.18	
2.0	191.43	171.32	151.21	131.10	111.11	93.56	

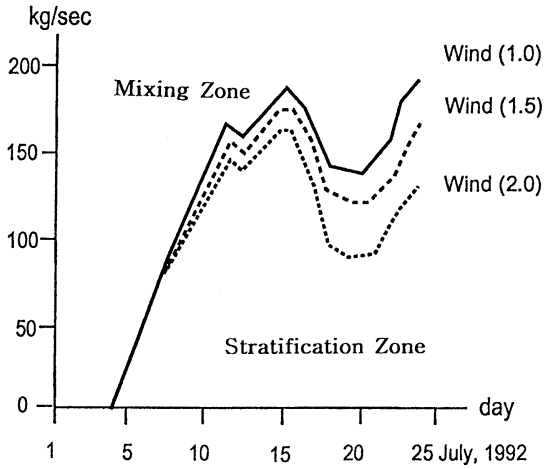

Fig. 6. Potential energy anomaly variation from 5 July to 23 July (ε =0.014). The number of ( ) indicated wind speed intensity of ratio of wind at sea surface and wind at land.

increases until 15 July. However, during the second spring tidal period from 16 to 19 July, the stratification decreases by strong tidal current amplitude although the current energy could not overcome the total potential energy caused by the sea surface heating. From the figure, we found that stratification continually sustained in the observation period from 5 to 23 July. The patterns of other energy variations following other ε values, which were not shown in this paper, should resemble at of ε =0.014, although the amount of total energy might be different during the same periods.

From the results, we supposed that ε -value ranged from 0.010 to 0.014 and from 5 or 6 July and the stratification had been started by the sea surface heating. It was emphasized that the strong sea surface heating in summer permitted only a short time of the vertically well mixed pattern and it might be less than one week based on the rate of energy variations.

Acknowledgements

This work was supported by Research Center for Ocean Industrial Development, National Fisheries Univ. of Pusan designated by KOSEF, in 1992.

References

BOWDEN, K. F. (1983): Physical Oceanography of Coastal Water. John Wiley & Sons Inc., Brisbane, 302 p.

ELLIOTT, A. J. and T. CLARKE (1991): Seasonal stratification in the northwest European Shelf Seas. Continental Shelf Research, **11**, 467–492.

GRIFFIN, D. A. and P. H. Leblond (1990): Estuary/ocean exchange controlled by spring-neap tidal mixing. Estuarine, Coastal and Shelf Science, **30**, 275–297.

GILL, A. E. (1982): Atmosphere-Ocean Dynamics. Academic Press, Oxford, 662 p.

IMANUKI, A. (1982): Turbulence and Atmosphere. Tokyo Press, Tokyo, 191 p.

LEE, J. C. (1992): Multidisciplinaly oceanographic studies in Deukryang Bay, Korea. 2nd International Conference Reports, Research Center for Ocean Industrial Development, Korea, 3–4.

LARGIER, J. L. and S. TALJAARD (1991): The dynamics of tidal intrusion, retention, and removal of seawater in a Bar-Built Estuary. Continental Shelf Research, **33**, 325–338.

MACKAY, H. M. and E. H. SCHUMANN (1990): Mixing and circulation in the Sundays River estuary, South Africa. Estuarine, Coastal and Shelf Science, **31**, 203–216.

SAMARASINGHE, J. R. de Silva (1989): Transient salt-wedges in a tidal gulf: criterion for their formation. Estuarine, Coastal and Shelf Science, **28**, 129–148.

SIMPSON, J. H. and D. BOWERS (1981): Models of

stratification and frontal movement in shelf seas. Deep Sea Research, **28**A, 727–738.

SIMPSON, J. H. and J. R. HUNTER (1974): Fronts in Irish Sea. Nature, **250**, 404–406.

TAKEOKA, H, H. AKIYAMA and T. KIKUCHI (1993): The Kyucho in the Bungo Channel, Japan "Periodic intrusion of oceanic warm water". Journal of Oceaography, **49**, 369–382.

YANAGI, T. (1980): Variability of the constant flow in Osaka Bay. Journal of the Oceanographical Society of Japan, **36**, 246–252.

YANAGI, T (1981): Heat budget of Uwajima Bay. Umi to Sora (Sea and Sky), **58**, 13–20 (in Japanese).

YANAGI, T and H. TAMARU (1990): Temporal and spatial variation in a tidal front. Continental Shelf Research, **7**, 61–627.

Received December 24, 1995
Accepted March 22, 1996